

Temporal statistical analysis of laser speckle images and its application to retinal blood-flow imaging

Haiying Cheng^{1*}, Yumei Yan, and Timothy Q. Duong^{2*}

Yerkes Imaging Center and Department of Neurology, Emory University, Atlanta, Georgia, 30329, USA

* Corresponding authors: hcheng4@emory.edu; tduong@emory.edu.

Abstract: Temporal-statistical analysis of laser-speckle image (TS-LSI) preserves the original spatial resolution, in contrast to conventional spatial-statistical analysis (SS-LSI). Concerns have been raised regarding the temporal independency of TS-LSI signals and its insensitivity toward stationary-speckle contamination. Our results from flow phantoms and *in vivo* rat retinas demonstrated that the TS-LSI signals are temporally statistically independent and TS-LSI minimizes stationary-speckle contamination. The latter is because the stationary speckle is “non-random” and thus non-ergodic where the temporal average of *stationary* speckle needs not equal its spatial ensemble average. TS-LSI detects blood flow in smaller blood vessels and is less susceptible to stationary-speckle artifacts.

©2008 Optical Society of America

OCIS codes: (170.6480) Speckle; (170.3880) Medical and Biological Imaging; (170.4470) Ophthalmology

References and links

1. J. D. Briers and A. F. Fercher, "Retinal blood-flow visualization by means of laser speckle photography," *Invest. Ophthalm. Vis. Sci.* **22**, 255-259 (1982).
2. A. K. Dunn, H. Bolay, M. A. Moskowitz and D. A. Boas, "Dynamic imaging of cerebral blood flow using laser speckle," *J. Cereb. Blood Flow Metab.* **21**, 195-201 (2001).
3. A. F. Fercher and J. D. Briers, "Flow Visualization by means of Single-Exposure Speckle Photography," *Opt. Commun.* **37**, 326-330 (1981).
4. H. Cheng, Q. Luo, Q. Liu, Q. Lu, H. Gong and S. Zeng, "Laser speckle imaging of blood flow in microcirculation," *Phys. Med. Biol.* **49**, 1347-1357 (2004).
5. Q. Liu, Z. Wang and Q.M. Luo, "Temporal clustering analysis of cerebral blood flow activation maps measured by laser speckle contrast imaging," *J. Biomed. Opt.* **10**, 024019 (2005).
6. B. M. Ances, J. H. Greenberg and J. A. Detre, "Laser doppler imaging of activation-flow coupling in the rat somatosensory cortex," *Neuroimage* **10**, 716-723 (1999).
7. J. D. Briers, G. Richards and X. W. He, "Capillary blood flow monitoring using laser speckle contrast analysis (LASCA)," *J. Biomed. Opt.* **4**, 164-175 (1999).
8. A. Serov, W. Steenbergen and F. de Mul, "Laser Doppler perfusion imaging with a complimentary metal oxide semiconductor image sensor," *Opt. Lett.* **27**, 300-302 (2002).
9. H. Cheng, Q. Luo, S. Zeng, S. Chen, J. Cen and H. Gong, "Modified laser speckle imaging method with improved spatial resolution," *J. Biomed. Opt.* **8**, 559-564 (2003).
10. P. C. Li, S. L. Ni, L. Zhang, S. Q. Zeng and Q. M. Luo, "Imaging cerebral blood flow through the intact rat skull with temporal laser speckle imaging," *Opt. Lett.* **31**, 1824-1826 (2006).
11. W. Luo, Z. Wang, P. Li, S. Zeng and Q. Luo, "A modified mini-stroke model with region-directed reperfusion in rat cortex," *J. Cereb. Blood Flow Metab.* advance online publication (2007).
12. Z. Wang, P. Li, W. Luo, S. Chen and Q. Luo, "Peri-infarct temporal changes in intrinsic optical signal during spreading depression in focal ischemic rat cortex," *Neurosci. Lett.* **424**, 133-138 (2007).
13. A. C. Volker, P. Zakharov, B. Weber, F. Buck and F. Scheffold, "Laser speckle imaging with an active noise reduction scheme," *Opt. Express* **13**, 9782-9787 (2005).
14. T. M. Le, J. S. Paul, H. Al-Nashash, A. Tan, A. R. Luft, F. S. Sheu and S. H. Ong, "New insights into image processing of cortical blood flow monitors using laser speckle imaging," *IEEE Trans. Med. Imaging* **26**, 833-842 (2007).

15. P. Zakharov, A. Volker, A. Buck, B. Weber and F. Scheffold, "Quantitative modeling of laser speckle imaging," *Opt. Lett.* **31**, 3465-3467 (2006).
16. H. Cheng and T. Q. Duong, "Simplified laser-speckle-imaging analysis method and its application to retinal blood flow imaging," *Opt. Lett.* **32**, 2188-2190 (2007).
17. R. Bonner and R. Nossal, "Model for Laser Doppler Measurements of Blood-Flow in Tissue," *Appl. Opt.* **20**, 2097-2107 (1981).
18. J. C. Ramirez-San-Juan, R. Ramos-Garcia, I. Guizar-Iturbide, G. Martinez-Niconoff and B. Choi, "Impact of velocity distribution assumption on simplified laser speckle imaging equation," *Opt. Express* **16**, 3197-3203 (2008).
19. J. W. Goodman, *Statistical Optics* (Wiley series in Pure and Applied Optics, 1985).
20. C. E. Riva, J. E. Grunwald and S. H. Sinclair, "Laser Doppler Velocimetry study of the effect of pure oxygen breathing on retinal blood flow," *Invest. Ophthalmol. Visual Sci.* **24**, 47-51 (1983).
21. Y. Li, H. Cheng and T. Q. Duong, "Blood-flow magnetic resonance imaging of the retina," *Neuroimage* **39**, 1744-1751 (2008).
22. J. W. Goodman, in *Laser Speckle and Related Phenomena* (Spring-Verlag, 1975).
23. J. D. Briers, "Time-varying laser speckle for measuring motion and flow," *Proc. SPIE* **4242**, 25-39 (2001).
24. H. Cheng, G. Nair, T. A. Walker, M. Kim, M. T. Pardue, P. M. Thule, P. M. Thule, D. E. Olson, T. Q. Duong, "Structural and Functional magnetic resonance imaging reveal multiple layers in retina," *Proc. Natl. Acad. Sci. USA* **103**, 17525-17530 (2006).

1. Introduction

Laser speckle imaging (LSI) is a simple and economical method to image surface blood flow (BF) in vivo [1-5]. The random speckle pattern is formed when coherent light is illuminated on a scattering surface. Movement of individual scatterers results in a change of speckle pattern, which is quantified as speckle contrast (K). A unique advantage of LSI is that BF image can be obtained in a snap shot without line scanning as is the case for laser Doppler flowmetry [6].

The most commonly used LSI analysis method utilizes spatial statistics (SS-LSI) in which a square matrix of 5×5 or 7×7 pixels is used to compute the speckle contrast image [2,7]. A disadvantage of SS-LSI is that it markedly compromises spatial resolution by size of the spatial kernel employed [7], making it less competitive against other BF imaging techniques [8]. An alternative approach based on temporal statistics (TS-LSI) has been proposed to preserve spatial resolution [9] in which the speckle contrast is computed using images acquired along a few time points without employing a spatial kernel. This approach has been applied to monitor changes in cerebral BF associated with stroke [10,11] and on intact skull [12]. However, questions have been raised regarding 1) whether the TS-LSI signals are temporally statistically independent [13,14] which would invalidate the approach, and 2) whether TS-LSI can minimize contamination due to stationary speckle [15]. Consequently, TS-LSI has not been widely utilized. In the present study, we re-derived a simplified TS-LSI framework to show that it has the same form as SS-LSI and validated the TS-LSI approach using a realistic flow phantom. Moreover, we utilized this approach was to demonstrate a novel application by imaging retinal BF in rats breathing air and oxygen. The temporal independence of the TS-LSI signals and its ability to minimize stationary speckle artifacts were investigated. Comparisons between TS-LSI and SS-LSI were made.

2. Framework of TS-LSI

We recently introduced a simplified SS-LSI method to image blood flow, which can be described as [16]:

$$T/\tau_c = 1/K_s^2 \quad (1)$$

where K_s is the speckle contrast in the spatial dimension, τ_c is the light coherence time, and T is the CCD camera exposure time. T/τ_c is proportional to the mean velocity [17] and generally taken as the measured BF index. This method was independently verified by another group [18].

The TS-LSI method can be described as [9],

$$1/N_t = \langle I \rangle^2 / [\langle I^2 \rangle - \langle I \rangle^2] \quad (2)$$

where $\langle I \rangle$ and $\langle I^2 \rangle$ are the mean and mean-square values of time-integrated speckle intensities during the time interval t for a specific pixel, and $1/N_t$ is proportional to the mean velocity of the scattering particles. Equation (2) can be rewritten as,

$$1/N_t = \bar{I}^2 / \sigma^2 = 1/K_t^2 \quad (3)$$

where K_t is the speckle contrast in the time dimension, \bar{I} is the mean intensity and σ is its variations during time interval t .

Comparison of Eqs (1) and (3) showed that the TS-LSI and SS-LSI methods have the same form. An advantage of TS-LSI is that it preserves the original spatial resolution, in contrast to SS-LSI which degrades spatial resolution by a 5x5 or 7x7 pixel kernels. A disadvantage of TS-LSI is that it has lower temporal resolution compared to SS-LSI because a few time points are needed to derive BF images although analysis using a moving time window can be employed to preserve its temporal resolution with some “temporal smoothing.” Thus, depending on the types of studies, one method may be preferred over the other.

3. Validation of TS-LSI

To validate the TS-LSI method, flow phantoms were studied. Intralipid (2%) solution is flowed in a polyethylene tube (0.58 mm inner diameter) from 0 to 10 mm/s (mean velocity) in steps of 1 mm/s driven by a digital syringe pump. LSI was performed using a 785-nm laser diode with $\Delta\lambda$ of ~1 nm and a modified video imaging system (Imager 3001, Optical imaging), operating at 25 Hz, 4x4 μm resolution, and 10-ms camera exposure time T . The CCD camera pixel resolution was 7.4x7.4 μm . The objective lens consisted of a tandem of 50 mm, 13.5mm Nikon lens, 2X converter lens and a custom-designed lens for the rat eye. The system magnification was 1.78. The f-number was 2.2. Under our experimental conditions, TS-LSI typically requires 15 frames to derive reliable blood-flow image. For comparison herein with SS-LSI analysis which used a 5x5 spatial kernel, 25 frames were employed for TS-LSI analysis. A total of 300 frames were acquired. Both analyses were performed on the same data sets. Five sets of measurements were repeated for each flow condition.

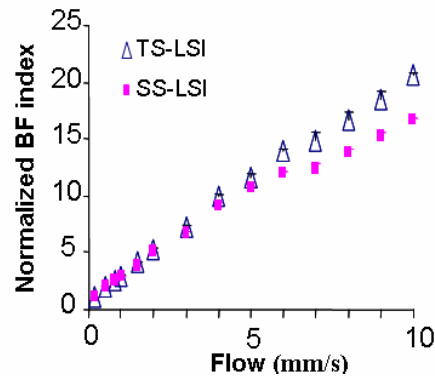


Fig. 1. Normalized blood flow indices calculated using temporal statistics (TS-LSI) and spatial statistics (SS-LSI) versus input flow velocities. Each data point represents five repeated measurements. Error bars are standard deviations. The linear correlation coefficients were 0.9956 and 0.9832 for TS-LSI and SS-LSI respectively.

Figure 1 shows the results of TS-LSI and SS-LSI analysis of the same flow-phantom data. Both TS-LSI and SS-LSI showed high correlation with the input flow rate, demonstrating the validity of the TS-LSI. At low flow rate (0-5 mm/s), TS-LSI and SS-LSI were essentially

identical. At high flow (5-10 mm/s), TS-LSI yielded better linear correlation with input flow. TS-LSI results are consistent with a previous report [9] in which a porcelain plane was driven by a stepping motor to simulate in-plane motion which has different characteristics than BF [7]. Thus, TS-LSI is applicable to both rigid in-plane motion and flow.

A concern has been raised regarding the temporal independence of TS-LSI analysis [13,14] – that is the speckle signals obtained along the time domain may be correlated. Consider a typical laser diode with a wavelength ranging from 600-800 nm and $\Delta\lambda$ of 1 nm, the coherence time $\tau_c = \bar{\lambda}^2 / (c\Delta\lambda) \sim 10^{-12}$ s. For a typical camera exposure time T of 5 to 20 ms, the minimal time interval between sequential image acquisitions is much larger than τ_c and thus the speckle signals along the time dimension are uncorrelated and thus statistically independent [19]. Thus, it is not necessary to disperse the laser beam by passing it through a rotating diffuser to achieve temporally statistically independent images [13]. Our phantom results support this conclusion.

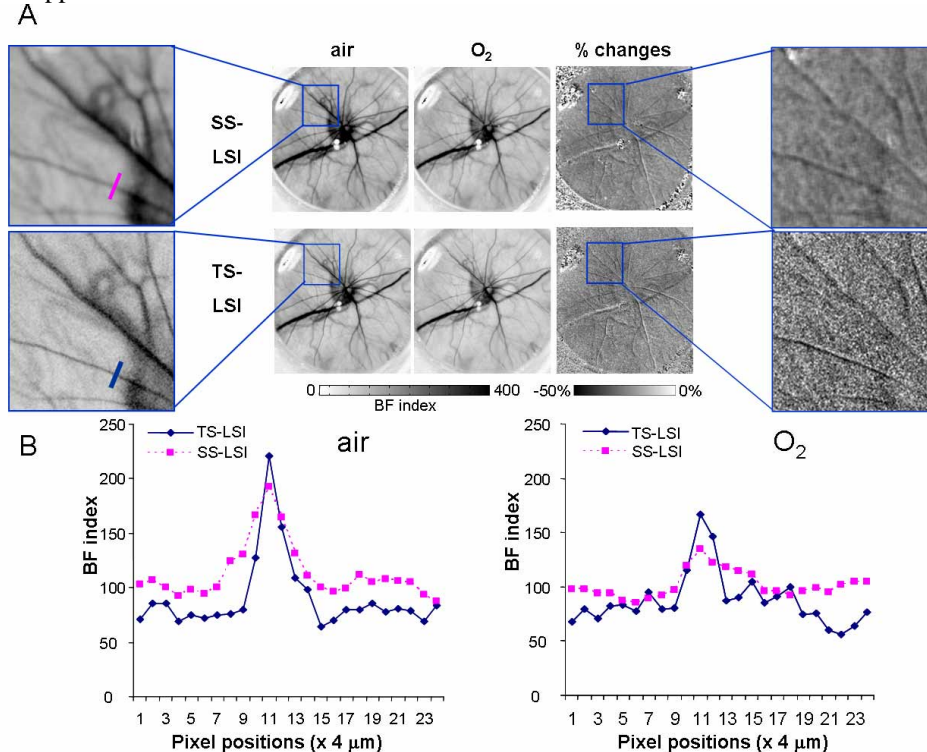


Fig. 2. (a). Spatial statistical (SS-LSI) and temporal statistical (TS-LSI) analysis of the retinal blood-flow images associated with air or oxygen breathing and their percent-change images. Blood-flow images are in arbitrary unit. The non-expanded image area is 4.5×4.5 mm. TS-LSI preserves high spatial resolution compared to SS-LSI but has lower signal-to-noise ratio as expected. SS-LSI and TS-LSI were calculated from the same data set of 300 frames. (b) A blood-flow profile across a blood vessel when the animal breathed air (left) or O₂ (right).

To demonstrate an application of TS-LSI, rat retinal BF was imaged in which the animal breathed air for 3 mins followed by oxygen for 3 mins. Three rats were anesthetized under ~1% isoflurane, mechanically ventilated and paralyzed with pancuronium bromide (1 mg/kg, ip). End-tidal CO₂, heart rate, arterial oxygen saturation and rectal temperature were monitored and maintained within normal physiological ranges. SS-LSI and TS-LSI were calculated from the same data sets (300 frames during air and 300 frames during oxygen). Two to four sets of measurements were repeated for each animal.

Figure 2(a) shows the TS-LSI and SS-LSI analysis of a rat retina. For each effectively time point, TS-LSI was computed using 25 consecutive frames without using a spatial kernel and SS-LSI was computed using a 5×5 spatial kernel followed by averaging 25 time points (the total acquisition time were the same). As expected, TS-LSI retains the original spatial resolution, whereas SS-LSI substantially degrades the spatial resolution. The signal-to-noise ratios (SNR), computed by taking the standard deviation along the time dimension of the time series data, were 17 for TS-LSI and 85 for SS-LSI – a difference of a factor of 5. This is because low-resolution SS-LSI derived by 1 frame using 5×5 pixel kernel had the same SNR as the high-resolution TS-LSI derived by 25 frames. The SNR of SS-LSI with 25 averages was thus 5 times higher than that of TS-LSI. This was also verified by analysis using a 7×7 and 9×9 kernels.

Following oxygen breathing, whole-retina BF decreases 20-30% ($n = 3$) due to hyperoxia-induced vasoconstriction, consistent with blood-flow results obtained using laser Doppler flowmetry [20] and magnetic resonance imaging [21, 24]. The blood-flow percent change map by TS-LSI had considerably higher spatial resolution and thus allowed detection of blood flow changes in smaller vessels. Although there are regional differences, whole-retina BF reductions are not statistically different between the two methods ($P > 0.05$), further supporting the validity of TS-LSI. Improved spatial resolution with TS-LSI is also evident in the BF profiles taken across a single vessel under air and oxygen breathing (Fig. 2(b)). As an aside, although it was not needed to detect steady-state oxygen responses herein, analysis using a moving time window can be employed to preserve high temporal resolution of TS-LSI to allow real-time monitoring of visually evoked BF changes, albeit some “temporal smoothing.”

4. Minimization of stationary speckle

Another concern is whether TS-LSI can minimize artifacts arising from stationary speckle. Our experimental setup allows this hypothesis to be tested. Figure 3(a) illustrates a source of this artifact. When the laser beam from the optical fiber is splitted, with half illuminating the object of interest and the other “unused” half illuminating a rough static surface, the latter signal is also recorded on the CCD camera and thus contaminates the speckles of the object of interest. This manifests into bright dots (arrows) on the retinal image obtained using SS-LSI (Fig. 3(b)). When the rough static surface (rough black cloth) is changed to a smooth surface (smooth black paper), the artifacts on the retinal image were less severe, but not completely eliminated in SS-LSI. However, when the same data were analyzed with TS-LSI, the artifacts were eliminated for both smooth and rough surface (Fig. 3(c)), demonstrating a unique feature of TS-LSI. Similarly, the optical fiber reflected off the corneal surface and appeared as a ring on the retinal image in SS-LSI (arrowheads). This artifact was essentially eliminated in TS-LSI.

We propose the following explanation. If the roughness of the static surface exceeds the laser coherence length ($c \times \tau_c \sim 0.3$ mm) as is the case of the rough static surface, the light coming off this surface became non-coherent and is detected by the camera. For SS-LSI, flow information is derived using spatial statistics and the non-coherent light from the static surface mixes with the speckles of the object of interest, resulting in dots on the retinal images [22]. For TS-LSI, however, no spatial statistical analysis is performed and, as these non-coherent light is temporally stable (as is the case by definition of a static object, albeit the presence of noise), little or no artifacts are registered on the retinal image. The same explanation also applies to the artifacts from the optical fiber (a static object). Indeed, TS-LSI has been successfully used to image cerebral BF through intact skull, a static scatterer [12]. Note that these observations may appear to violate the ergodic theorem which states that the temporal average of speckle should equal to its spatial ensemble average [23]. However, it is not the case. The ergodic process is only valid for random speckle arising from moving objects. In the case of the stationary object, its speckle is static (not temporally varying) and thus non-

ergodic. Consequently, the temporal average of stationary speckle needs not equal its spatial ensemble average [23]. It can thus be generalized that TS-LSI has the unique feature of being less susceptible to artifacts from stationary speckle and this feature does not violate the ergodic theorem.

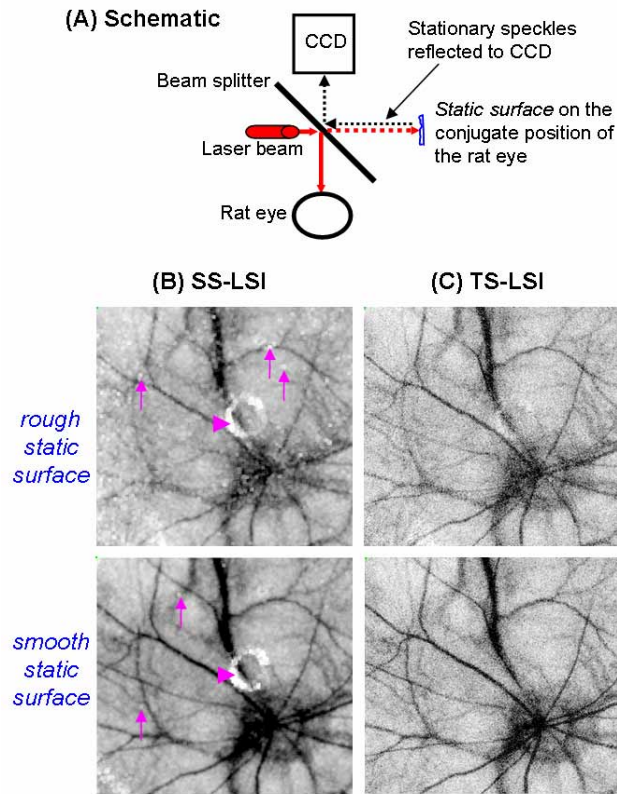


Fig. 3. (a). Schematic of stationary speckle artifacts. Half of the laser beam that passes through the beam splitter incidents on a static background. Light from the static background is reflected onto the camera and can contaminate the speckle images of interest. (b) Spatial statistical (SS-LSI) and (c) temporal statistical (TS-LSI) analysis of retinal blood-flow images obtained with a rough (rough black cloth) or smooth (smooth black paper) surface. Artifacts from the static surface (arrows) and optical fiber ring (arrowheads) were substantial in SS-LSI but were essentially eliminated in TS-LSI. SS-LSI and TS-LSI were calculated from the same data set of 50 frames. Image area is 3.5×3.5 mm.

5. Conclusion

This study demonstrates the validity of TS-LSI to calculate blood-flow images. TS-LSI speckles are temporally independent under typical *in vivo* experimental conditions. The equation of TS-LSI has the same form as that of SS-LSI. Although TS-LSI has poorer temporal resolution than SS-TSI as expected, it preserves high spatial resolution and is less susceptible to artifacts arising from stationary speckle. To minimize the impact of time penalty on TS-LSI, a smaller number of time frames can be used albeit lower signal-to-noise ratio and/or a moving time window analysis can be utilized to preserve high temporal resolution albeit some temporal “smoothing”.

Acknowledgments

This work is supported by the Department of Veterans Affairs (Career Development Award) and the NIH (NEI R01-EY014211) to TQD.